International Journal of Research in Engineering and Science (IJRES)
ISSN (Online): 2320-9364, ISSN (Print): 2320-9356
www.ijres.org Volume 10 Issue 12 ǁ December 2022 ǁ PP. 462-483

Melting and Nematic Phase Transitions of a Next Generation "Binary Liquid Crystal System (BLCS)" 5CB+7CB using Logger Pro.

Mathew C. Doran1 and Dipti Sharma (PhD) 2*
1 Undergraduate student, Emmanuel College, Boston, MA, USA
*2 Supervisor, Emmanuel College, Boston, MA, USA, * Corresponding Author: dsharmaphd@gmail.com*

ABSTRACT
Liquid Crystals (LCs) are important materials in the area of science, engineering, research and technology. Several technologies throughout the world can be seen using Liquid Crystals in Liquid Crystal Display (LCD) devices like smart TVs, watches and laptops. Our intention is to find some hidden effect of LCs that can be useful in LCDs when a binary mixture of LCs is used rather than just one. This research reports the thermal details of melting and nematic phase transitions of a Binary Liquid Crystal System (BLCS) of 5CB and 7CB mixed in 1:1 by weight ratio. We like to call this BLCS a next generation LC system as it shows very unique thermal behavior than its parent LCs. The thermal data are obtained using Differential Scanning Calorimetry (DSC). The details of DSC results are analyzed using Logger Pro. This next generation BLCS does not show crystallization in cooling when the parent LCs 5CB and 7CB show crystallization in cooling when run individually. This indicates an increase in Nematic Range when using this next generation BLCS which shows its significance in the LCD world.

KEYWORDS
Liquid Crystal (LC), Liquid Crystal Display (LCD), Binary Liquid Crystal System (BLCS), Next generation, Differential Scanning Calorimetry (DSC), LoggerPro, Phase transition, Melting, Nematic, Isotropic, Crystallization, Heat Flow, Specific Heat Capacity, Endothermic, Exothermic, Peak integrals, Integral, Enthalpy, Wing jump, Nematic Range, Thermal Behavior

---

Date of Submission: 11-12-2022 Date of acceptance: 26-12-2022

I. INTRODUCTION

In 1888 an Austrian physiologist Friedrich Reinitzer found that cholesteryl benzoate had two melting points, unlike any other compounds he had tested. It melted to a cloudy liquid at 145.5°C then melted again into a clear liquid at 178.5°C. After sending letters to concern Otto Lehmann with the phenomenon they concluded they were seeing crystallites in the cloudy liquid. The cloudy liquid was a liquid crystal. Studies by Lehmann showed that cholesteryl benzoate was clearly a fluid flowing liquid, but when looked at under a microscope displayed the ordered structure of a solid. [1]

Liquid crystal (LC) is a state of matter with properties between crystalline solids and conventional liquids, so a liquid crystal may bend or stretch while maintaining a crystal-like structure. If short range positional order is lost at the melting point but the orientational long range order is maintained, a liquid crystal phase is achieved, but this phase is not permanent as they could be completely solid, liquid, or gas as well. The typical liquid crystal phases seen in Figure 1 include Nematic (N), Smectic A (SmA), or Smectic C (SmC), where isotropic is complete melting to liquid phase and crystalline is solid. [2]

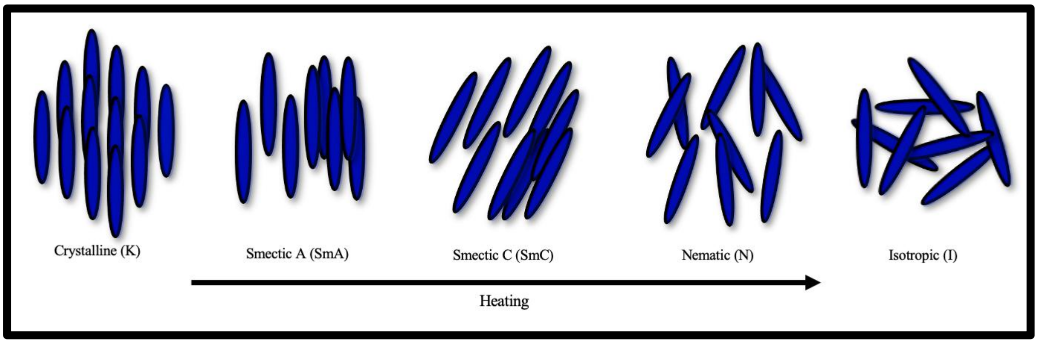

Figure 1. Progression of Liquid Crystal Phases during heating.

Liquid Crystals polarize light by transforming horizontal or vertical polarization into the other, like crystals, while still flowing like liquids. So electric fields can be used to change the orientation of liquid crystal particles and alter their effect on light based on the orientation of the liquid crystal phase. When applying an electric field to a thin layer of nematic LCs at 125°C, Reinitzer observed a pattern he called domains, that caused one of his colleagues, George H. Heilmeier to research a replacement of the cathode ray tube design for the television using liquid crystals. [3-4] This replacement technology is called Liquid Crystal Displays (LCDs) which are flat panel displays that use Liquid Crystals (LCs) to operate and are a massive technological leap from Light emitting diode (LEDs) and cathode ray tube devices. LCDs are able to be much thinner and consume much less energy because instead of emitting light, liquid crystals create images using a backlight (blocking light). In LCDs lit by a backlight, the pixels are switched on and off while using liquid crystals to rotate polarized light for color. A polarizing glass filter sandwiches each pixel with LCs front and back, the one in front is positioned at 90 degrees. Active-matrix LCDs have transistors at each pixel intersection, requiring less current to control a pixel's luminance. [5-8]

Other than optics, thermal techniques are also used to characterize LCs. Many studies surrounding the thermal behavior of 4-octyl-4-cyanobiphenyl (8CB) and 4-pentyl-4-cyanobiphenyl (5CB) liquid crystals show that they are the most popular LC molecules in modern day LCD devices. Due to the favorable thermodynamic conditions of each 8CB and 5CB's nematic phase transitions, studies on relative LC molecules like pentyl-oxy-cyanobiphenyl (5OCB) and nCB family members show that different uses of LCD devices could require different LC molecules based on the different thermal requirements of each of their nematic phase transitions. The studies show that along with 8CB and 5CB, 4-heptyl-4-cyanobiphenyl (7CB) is utilizable in reducing screen lag in LCD devices, and 4-hexyl-4-cyanobiphenyl (6CB) is effective in LCD screens at lower temperatures. [9-14] Differential scanning calorimetry (DSC) is a technique used to analyze and detect change in states in terms of exothermic and endothermic peaks or change in heat flow of the sample over a certain temperature change. Several studies can be seen on DSC using types of material including LCs. [9 -16]

Given the favorable features of 7CB's nematic phase transitions, the intention of this paper is to compare thermal behavior between LCD viable 5CB and 7CB molecules, with the phase transition behavior of an equal weight percent (1:1) Binary Liquid Crystal System (BLCS) of 5CB and 7CB. Furthermore, this paper focuses on the details of phase transitions of mixture of 5CB and 7CB LCs called Binary Liquid Crystal System (BLCS) for melting and nematic states. Logger Pro is used as a data analysis software for the results that is obtained from DSC by running BLCS in it. The results of BLCS found through DSC are amazing and show that BLCS can be considered as a next generation LCs for LCDs. The details of the results of BLCS focuses on its utility in LCDs.

EXPERIMENTS AND THEORY

Two pure, bulk samples of 4-pentyl-4-cyanobiphenyl (5CB) and 4-heptyl-4-cyanobiphenyl (7CB) liquid crystals seen in Figures 2 and 3 with molecular weights of 249.36 and 277.41 g/mol respectively, were added in equal amount to a new bottle, heated until they melted, mixed, and degassed for an hour. Then used as a binary mixture of 5CB and 7CB to be a next generation BLCS 5CB+7CB (1:1) for study.

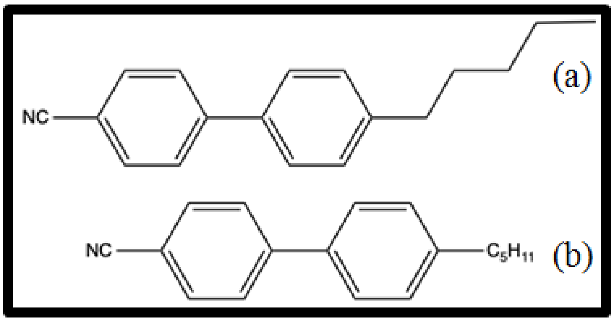

Figure 2. (a) Skeletal and (b) simplified chemical structure of 5CB LC.

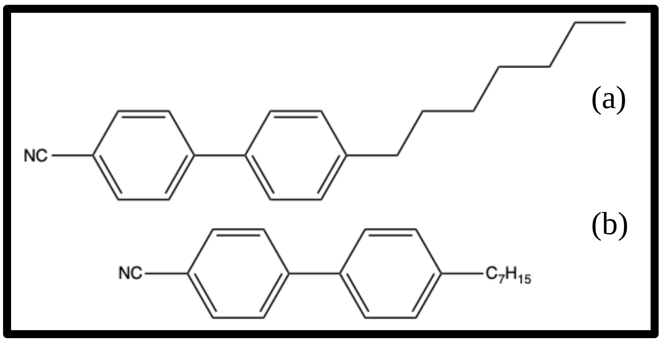

Figure 3. (a) Skeletal along with a (b) simplified chemical structure of 7CB LC.

This Binary system was then loaded into a Differential Scanning Calorimeter (DSC) from NETZSCH, DSC 214 Model that is at WPI's, chemistry and biochemistry department. Then this sample is heated and cooled from -30 °C to 101 °C and from 101 °C to -30 °C for three ramp rates as 5 °C/min, 10 °C/min and 20 °C/min. The results obtained from DSC were compared with the DSC results for its parents and it is found that 5CB and 7CB parents show sharp melting peaks in heating and sharp crystallization peaks in cooling along with appearance of Nematic peaks in heat and cool. Whereas the next generation BLCS shows a broad melting peak in heating and no crystallization in cooling.

The disappearance of crystallization peak in cooling makes this binary system useful in the real world of LCDs. The detailed thermal results of each peak and phases of 5CB+7CB binary mixture is shown in the result section. The theory in this paper is given below:

Heat Flow to a substance (dQ/dt) can be calculated as a function of temperature (T) and heating rate (dT/dt) using DSC technique through the relation between the mass (m) and specific heat capacity (Cp) of the substance,

$$\frac{dQ}{dT} = m * Cp * \frac{dT}{dt} - 1$$

Rearranging the first equation can provide the specific heat capacity of a substance, [17-20]

$$Cp = \frac{1}{m} * (\frac{dQ}{dt} / \frac{dT}{dt}) - 2$$

The change in Enthalpy (ΔH) representing the total internal energy change of the substance during heating and cooling, is the integration of a Cp Vs T graph represented by,

$$\Delta H = \int Cp \, dt - 3$$

The terms in these equations and their units are as follows: dQ/dt or Heat Flow is in Watts or J/s, after normalizing the heat flow it was in W/g giving the specific heat capacity units of J/g°C. Mass was measured in grams, time in seconds, and temperature in °C or K.

II. RESULTS

The data obtained from DSC are plotted with Logger Pro to see results of BLCS for all three-ramp heating and cooling rates. Figure 4 shows the DSC thermogram of the 5CB + 7CB LC mixture for three heating and cooling cycles at R= 5,10, and 20°C/min. The upward peaks represent endothermic, or energy absorbing, melting and nematic phase transitions in heating and the downward peaks denote the exothermic, or energy releasing nematic phase transitions in cooling. A slight increase in melting and heating nematic transitions is seen along with a decrease in cooling nematic transition temperatures.

In Figure 5, a rate isolated version of Figure 4 to show the HF Vs T of the LC mixture at R=5°C/min is shown. It shows a large upward endothermic peak at -20.23°C which represents the absorption of heat to melt the binary system from crystalline to nematic phase which is seen in the horizontal portion of the data after the melting peak. It shows an upward endothermic peak in heating that is much smaller in size at 42.33°C for the heating nematic to isotropic transition. The isotropic state is seen in the horizontal stretch of data after the heating nematic transition peak. The vertical part of the plot at 100°C shows when the calorimeter switched from heating to cooling. So, the LC mixture remained in the isotropic phase until it reached the cooling nematic transition temperature 39.41°C, represented by a downward exothermic peak and recorded in Table 1. The symbols used in Figures 5-13 are also detailed in Table 1.

Figure 6 is a version of Figure 4 that shows the HF Vs T of the LC mixture at R=10°C/min. It shows an upward endothermic peak at -16.49°C followed by the horizontal portion of data representing the nematic phase. There is another upward endothermic peak in heating that is much smaller at 43.27°C for the heating nematic to isotropic transition. The LC system remained in the isotropic phase until it reached the cooling nematic transition temperature 38.07°C as shown in Table 1, displayed by a downward exothermic peak.

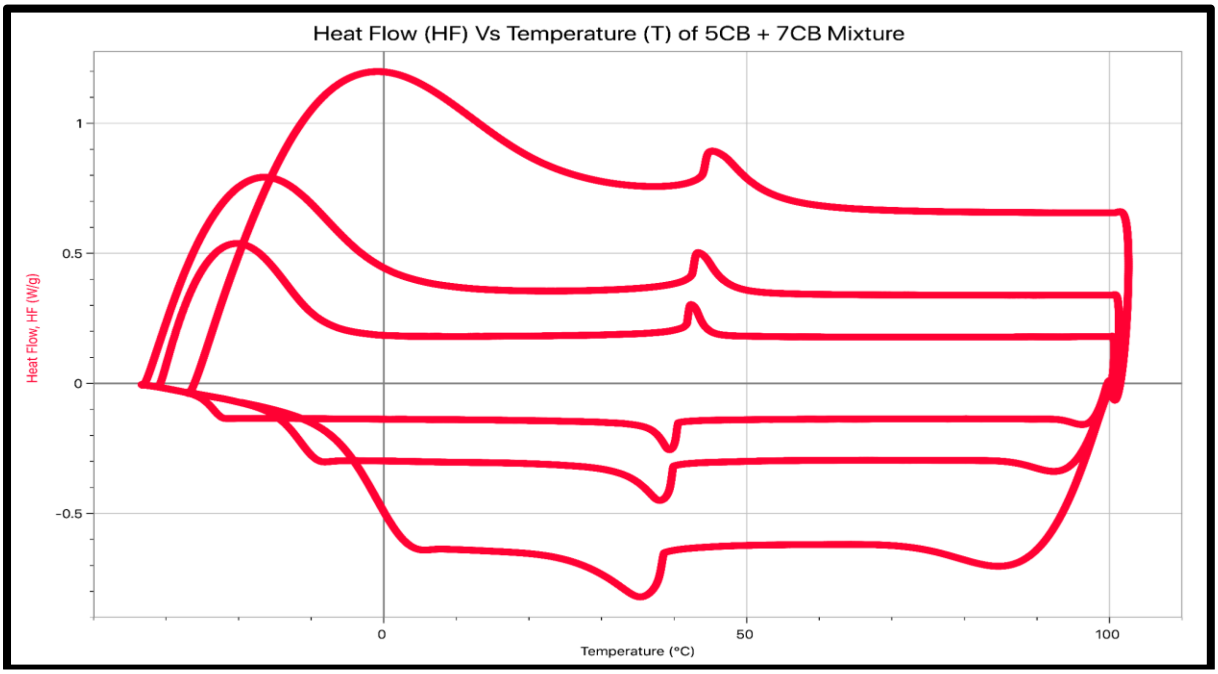

Figure 4. Heat Flow Vs Temperature plot for Melting (M) and Nematic (N) phase transitions of 5CB + 7CB BLCS at R= 5,10, and 20°C/min for heating and cooling.

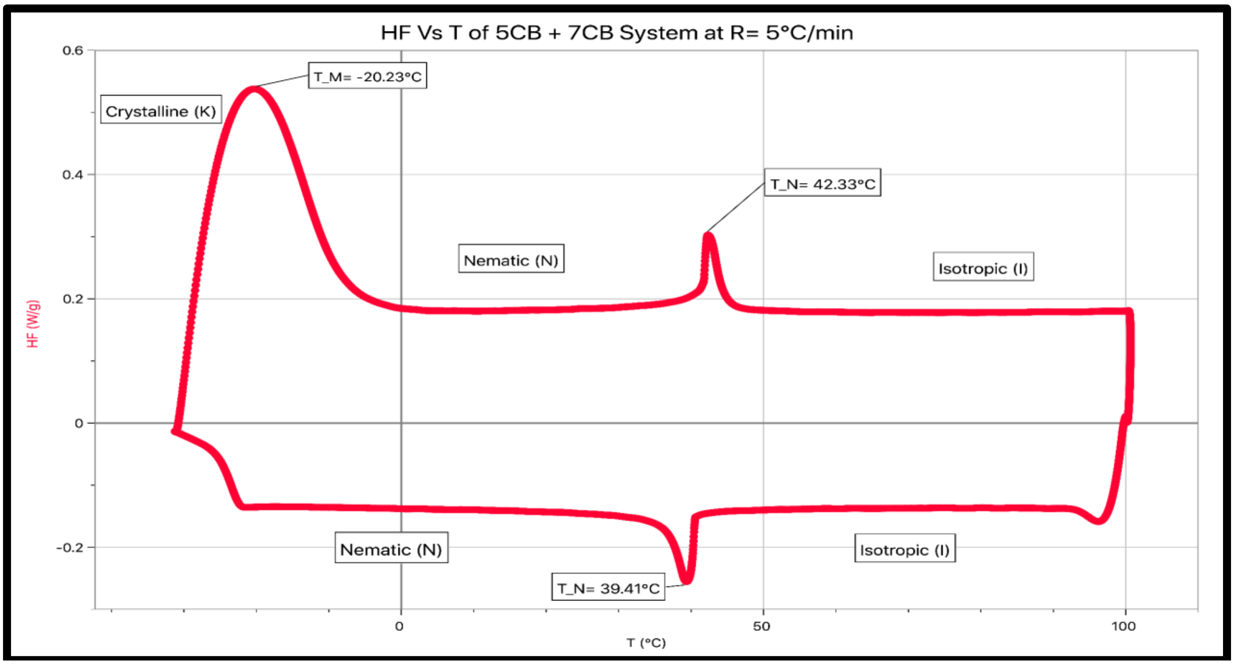

Figure 5. HF Vs T of 5CB + 7CB BLCS for one run of heating and cooling at R=5°C/min.

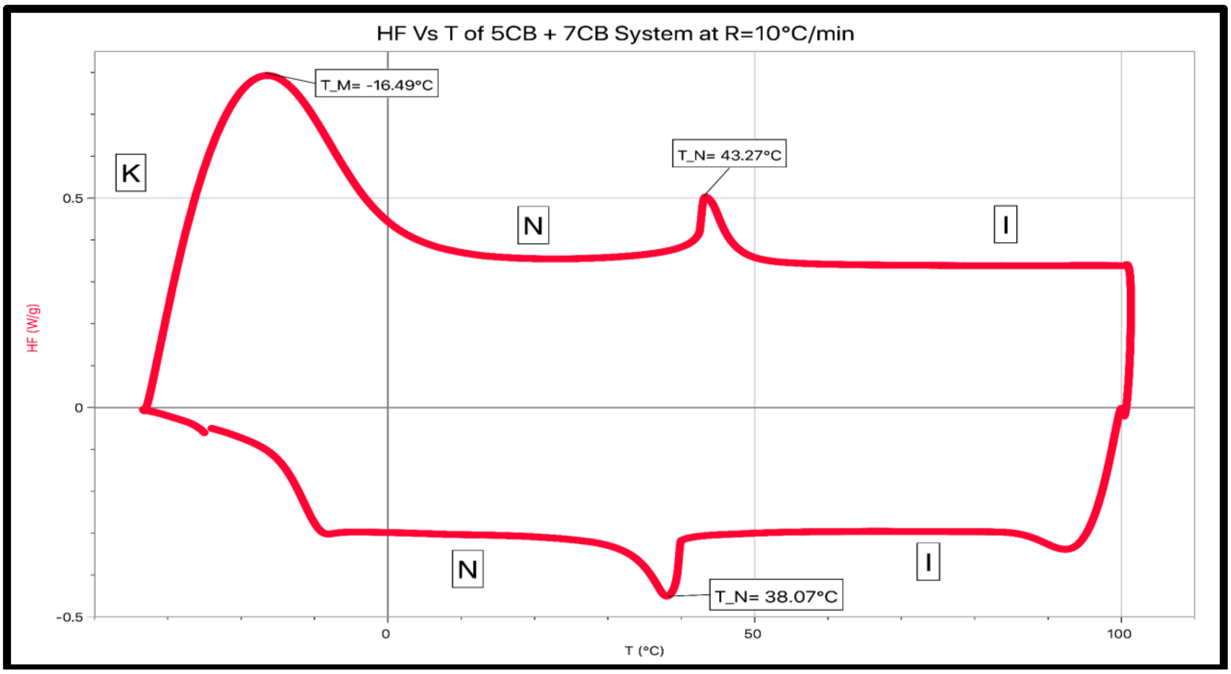

Figure 6. HF Vs T of 5CB + 7CB BLCS for one heating and cooling run at R=10°C/min.

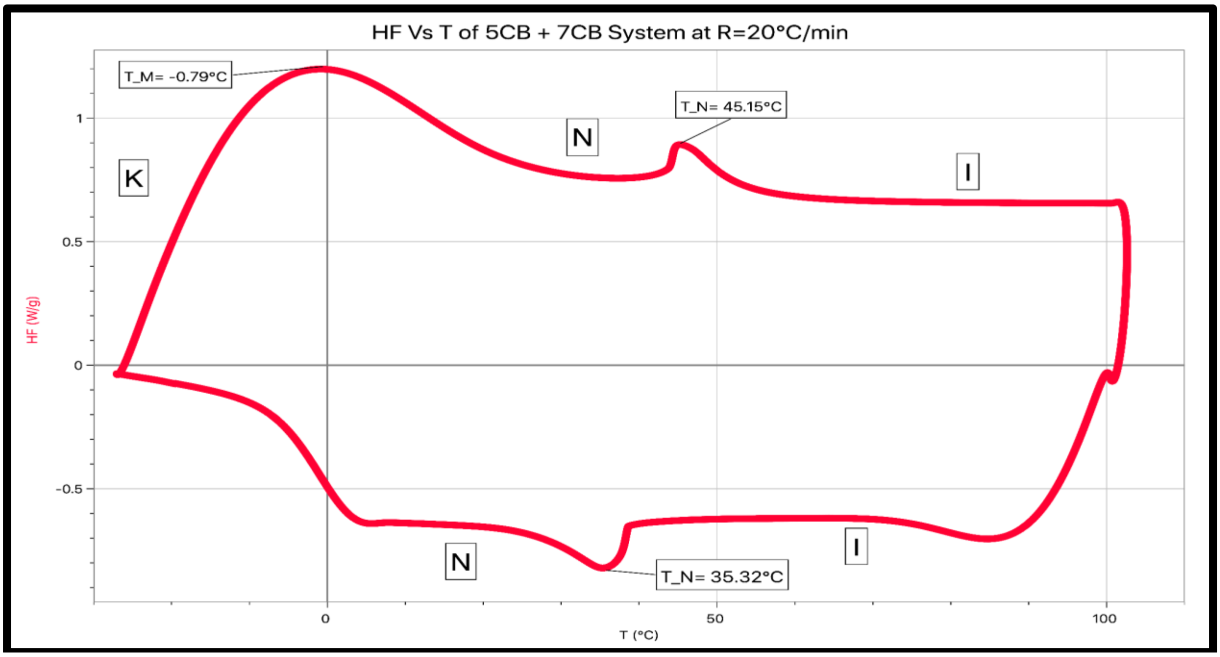

Figure 7. HF Vs T of 5CB + 7CB BLCS for one heating and cooling run at R=20°C/min.

Seen in Figure 7 is a version of Figure 4 to show just the HF Vs T of the LC mixture at R=20°C/min. The upward endothermic peak at -0.79°C represents the melting transition of the LC mixture. Another upward endothermic peak in heating at 45.15°C shows the heating nematic to isotropic transition. The binary LC system was in the isotropic phase until it reached the cooling nematic transition temperature at 35.32°C shown with an exothermic, downward peak. All transition temperatures are found in Table 1.

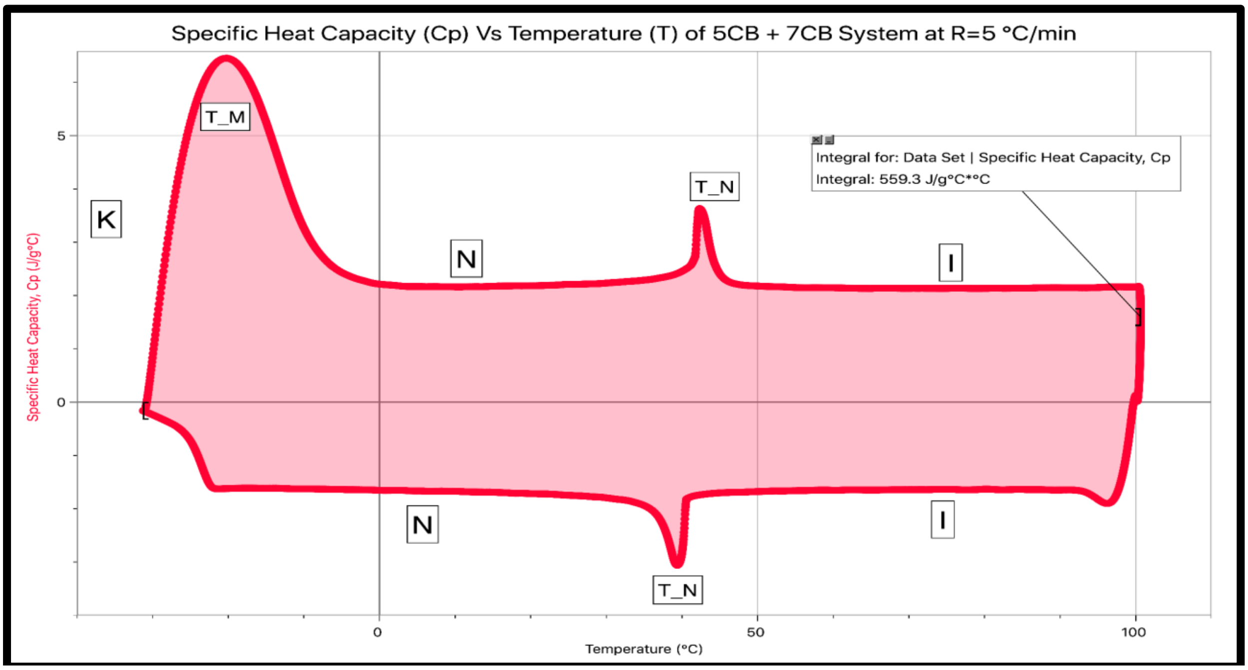

Figure 8. Specific Heat Capacity (Cp) Vs T plot for 5CB + 7CB BLCS at R=5°C/min. The shaded area represents the change in internal energy of the mixture during heating and cooling.

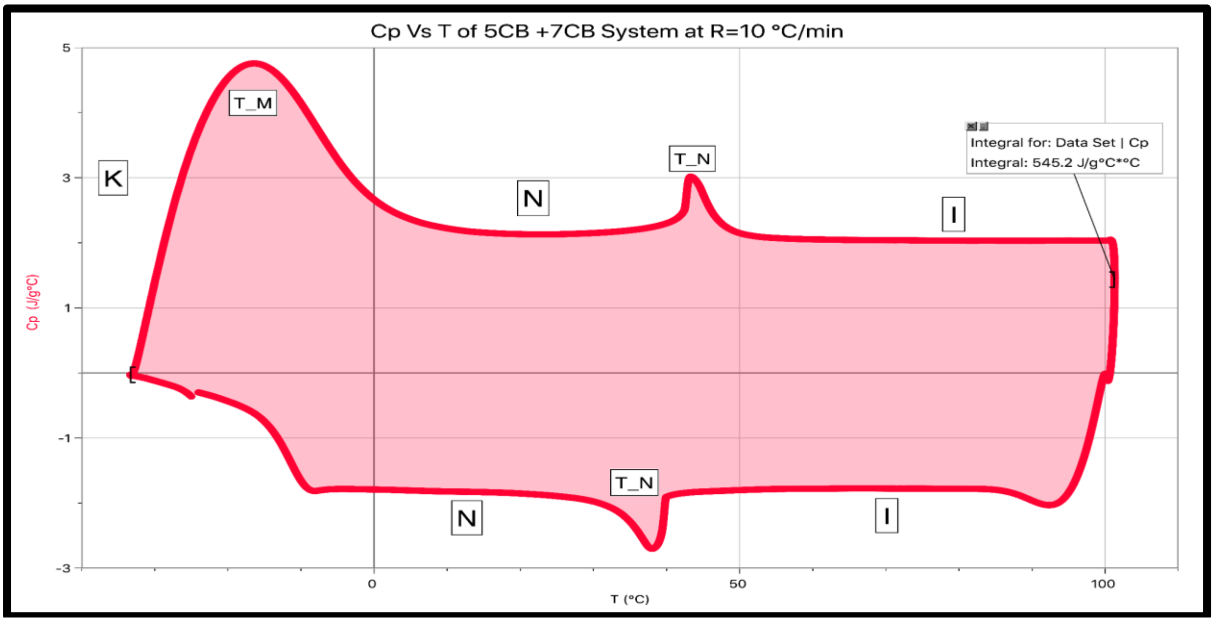

Figure 9. Cp Vs T plot for 5CB + 7CB BLCS at R=10°C/min. The shaded area represents the change in internal energy of the mixture during heating and cooling.

An approximation of the arrangement of liquid crystal molecules in the 5CB + 7CB mixture in terms of its change in internal energy during heating and cooling at R=5°C/min is seen in Figure 8. To do this, the specific heat capacity was plotted on the y-axis and the temperature on the x-axis. The pink shaded area shows the integral of the plot which represents the preservation or release of energy during the heating and cooling cycle. The amount of change in internal energy given was 559.3 J/g°C as seen in Figure 8.

Figure 9 approximates the arrangement of molecules in the binary mixture in terms of its change in internal energy during heating at R=10°C/min. The pink shaded area shows the integral of the plot which signifies the release or absorption of energy during heating and cooling which was given as 545.2 J/g°C, seen in Figure 9 and Table 1.

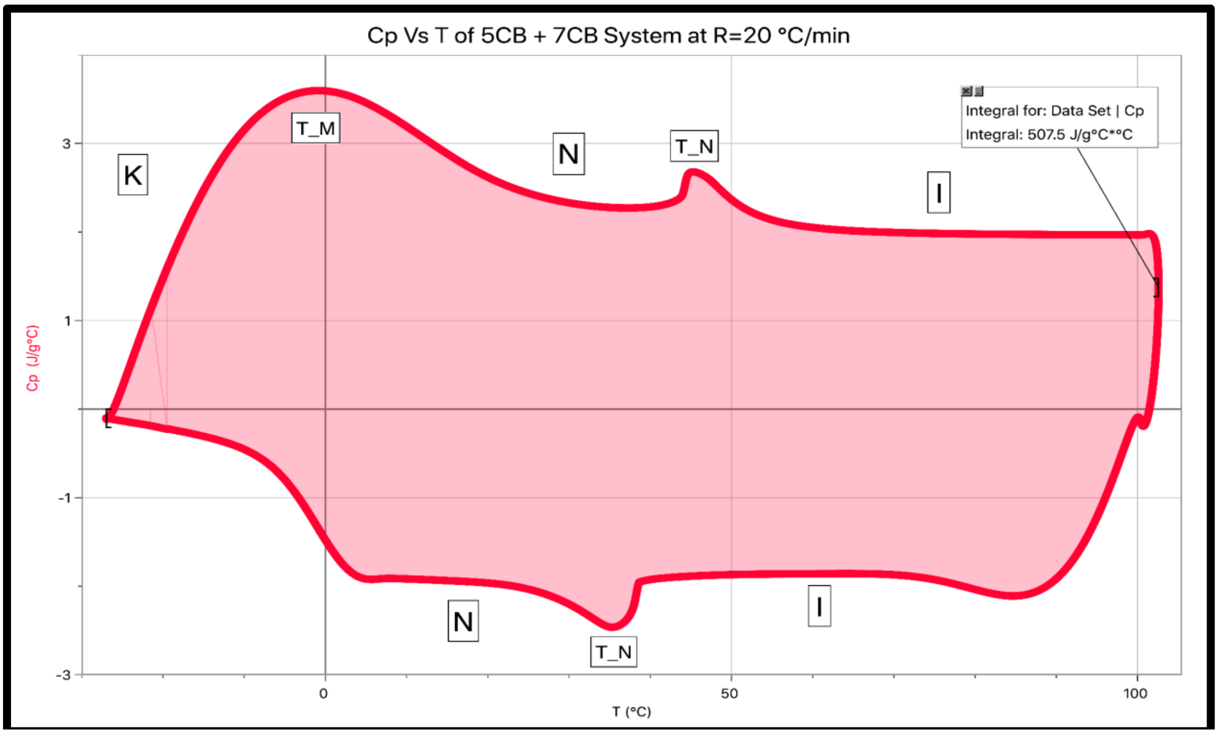

Figure 10. Cp Vs T plot for 5CB + 7CB BLCS at R=20°C/min. The shaded area represents the change in internal energy of the mixture during heating and cooling.

Figure 10 approximates the arrangement of molecules in the binary liquid crystal system in terms of the change in internal energy for heating at R=20°C/min. The pink shaded area shows the integral of the plot to show how much energy was used for phase transitions during heating and cooling and provided a value of 507.5 J/g°C as seen in Figure 10.

Within Figure 11, the Cp Vs T of the 5CB + 7CB mixture while heating at R=5°C/min separated into its heating and cooling scans is displayed. It is seen that the heating scan displayed two endothermic melting and nematic phase transition peaks whereas the cooling scan only provided one exothermic nematic transition peak and none for crystallization.

In Figure 12, the Cp Vs T of the BLCS while heating at R=10°C/min separated into heating and cooling is seen. The phase transition peaks at R=10°C/min are wider yet slightly closer than the peaks seen in Figure 8, so the nematic range decreases in heating and cooling as the ramp rate increases.

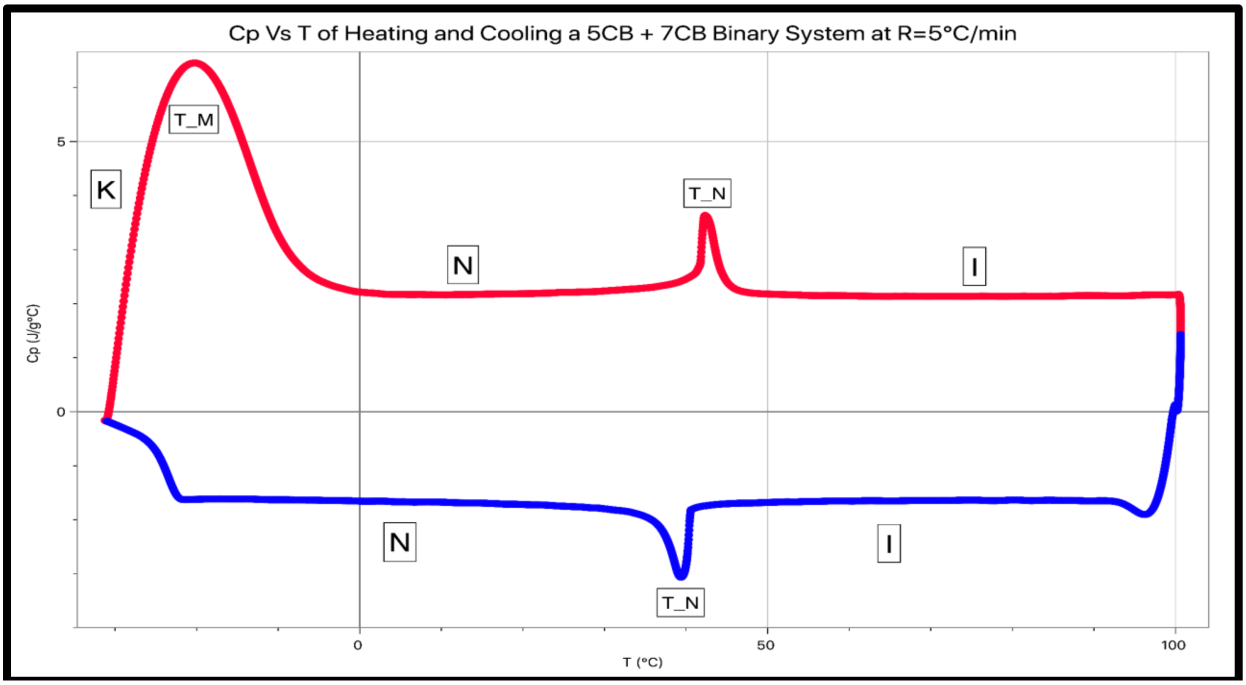

Figure 11. Cp Vs T plot for heating (red) and cooling (blue) a 5CB + 7CB BLCS at R=5°C/min.

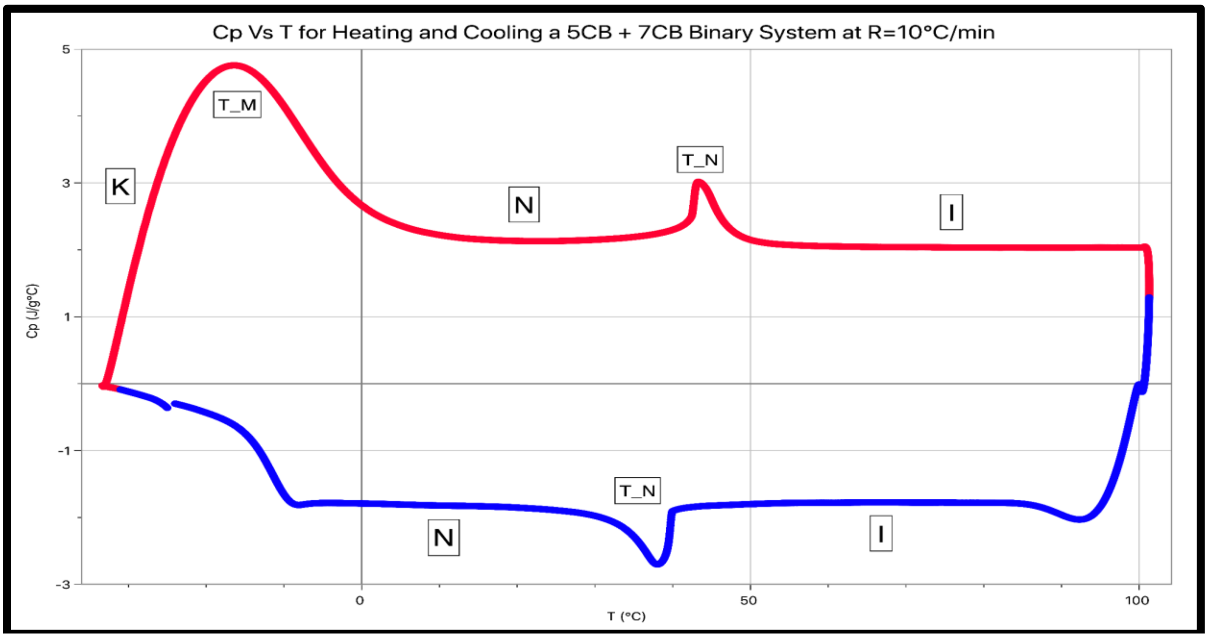

Figure 12. Cp Vs T plot for heating (red) and cooling (blue) a 5CB + 7CB BLCS at R=10°C/min.

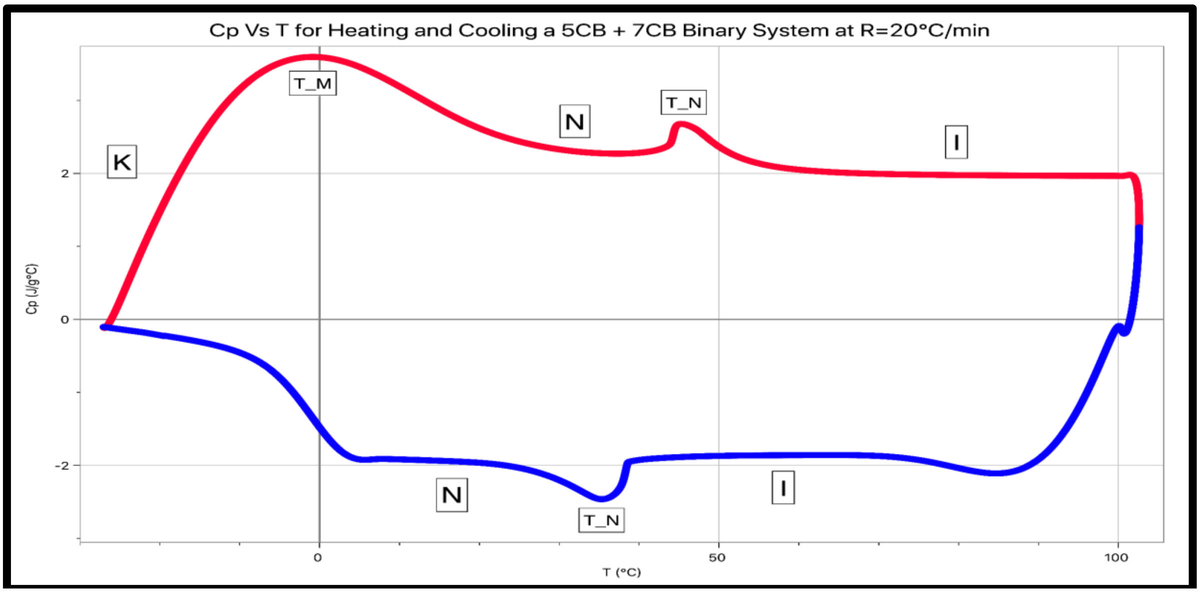

Figure 13. Cp Vs T plot for heating (red) and cooling (blue) a 5CB + 7CB BLCS at R=20°C/min.

Figure 13 shows the separate heating and cooling scans of Cp Vs T for the BLCS while heating at R=20°C/min. The phase transition peaks at R=20°C are even wider than R=10°C/min, but the nematic range is even smaller for both heating and cooling.

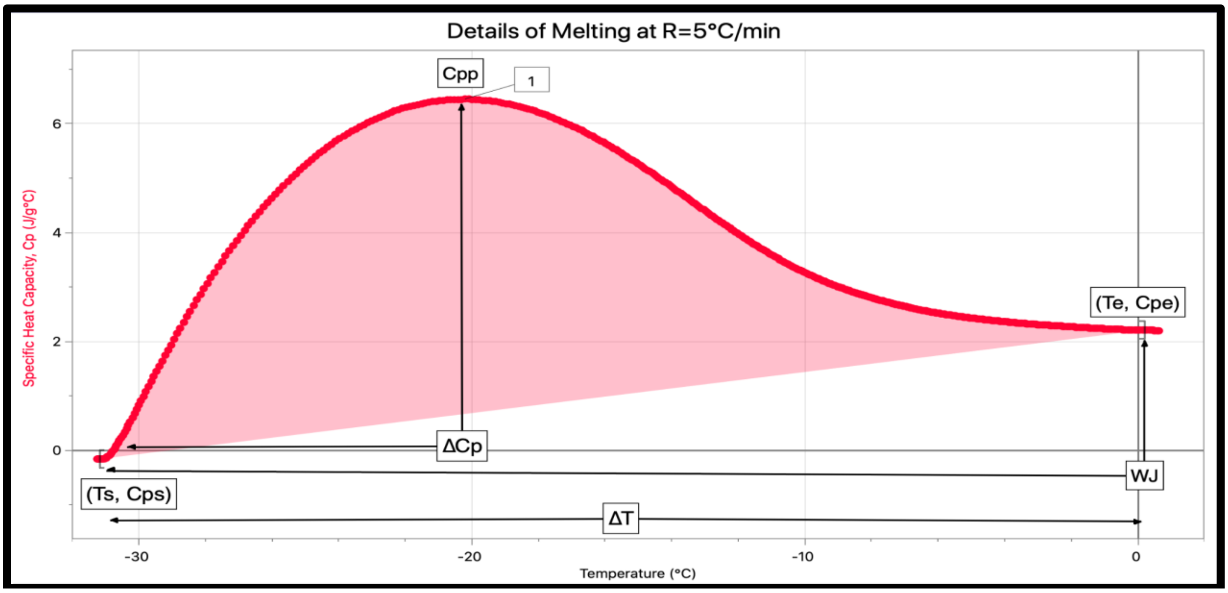

Figure 14. Cp Vs Temperature (T) for endothermic Melting peak of heating a 5CB + 7CB mixture at R=5°C/min. Details of T_s, T_e, ΔT, enthalpy, peak height and WJ can be found in Table 2.

Figure 14 shows the enlarged melting phase transition of the LC mixture in heating from Figure 8 and highlights details like starting and ending temperatures and specific heat capacities, wing jump and change in temperature of the melting phase transition at R=5°C/min. The symbols used in Figures 14-22 are detailed in Table 2. The pink area representing the peak integral gives the quantity of thermal energy absorbed by the LC sample in order to complete the melting transition. The amount of thermal energy needed to complete the melting transition to the nematic state at R=5°C/min was 91.99 J/g as seen in Table 2.

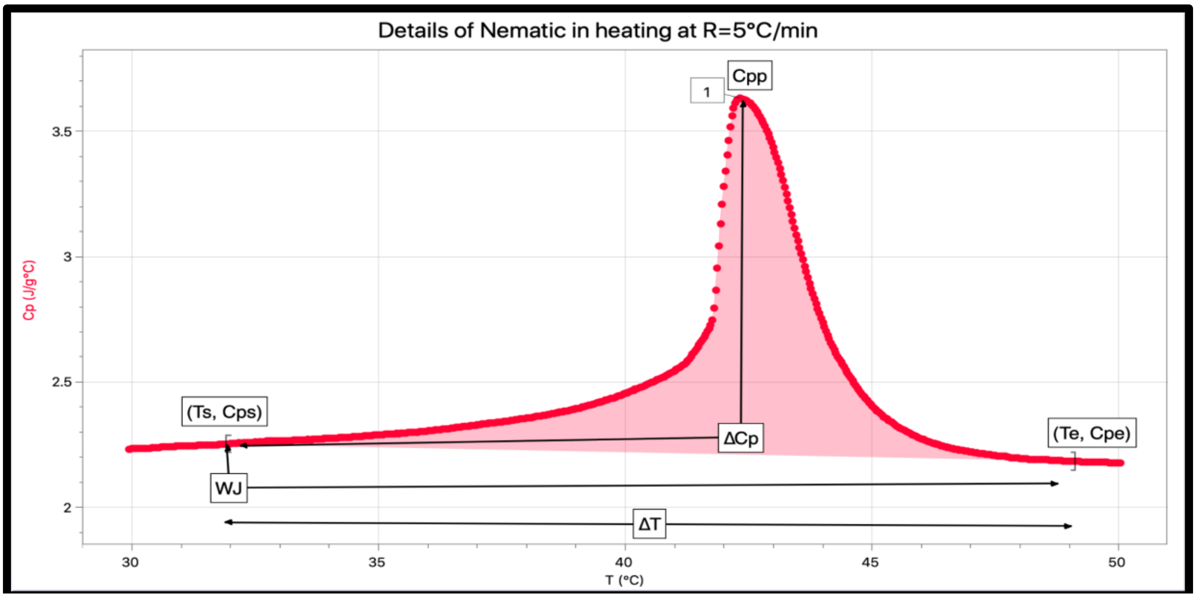

Figure 15. Cp Vs T for endothermic Nematic peak of heating a 5CB + 7CB mixture at R=5°C/min.

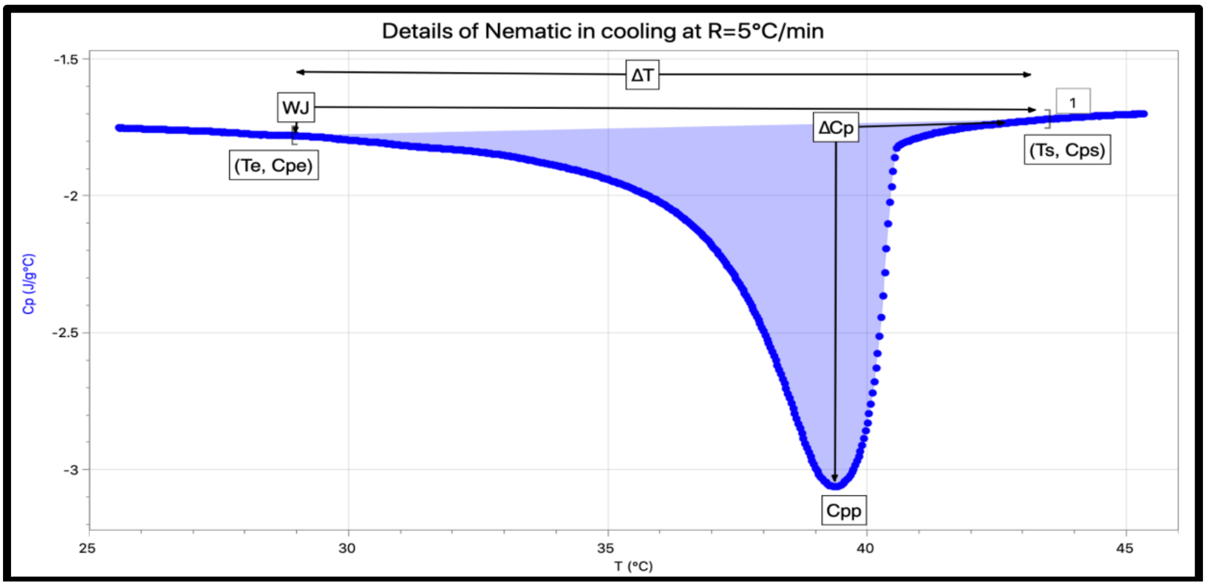

Figure 16. Cp Vs T for exothermic Nematic peak of cooling a 5CB + 7CB mixture at R=5°C/min.

Figure 15 is a zoomed-in plot of the nematic phase transition in heating from Figure 8 and highlights details like starting and ending temperatures and specific heat capacities, wing jump and change in temperature of the melting phase transition at R=5°C/min. The pink peak integral area gives 4.21 J/g as the quantity of thermal energy absorbed by the binary sample in order to complete the nematic transition at R=5°C/min seen in Table 3.

Figure 16 shows the magnified nematic phase transition of the LC mixture in cooling seen in Figure 5 and labels peak features like starting and ending temperatures and specific heat capacities, wing jump and change in temperature of the nematic phase transition at R=5°C/min. The blue area representing the peak integral gives the quantity of thermal energy released by the binary sample in order to complete the nematic transition as 4.3 J/g as seen in Table 4 .

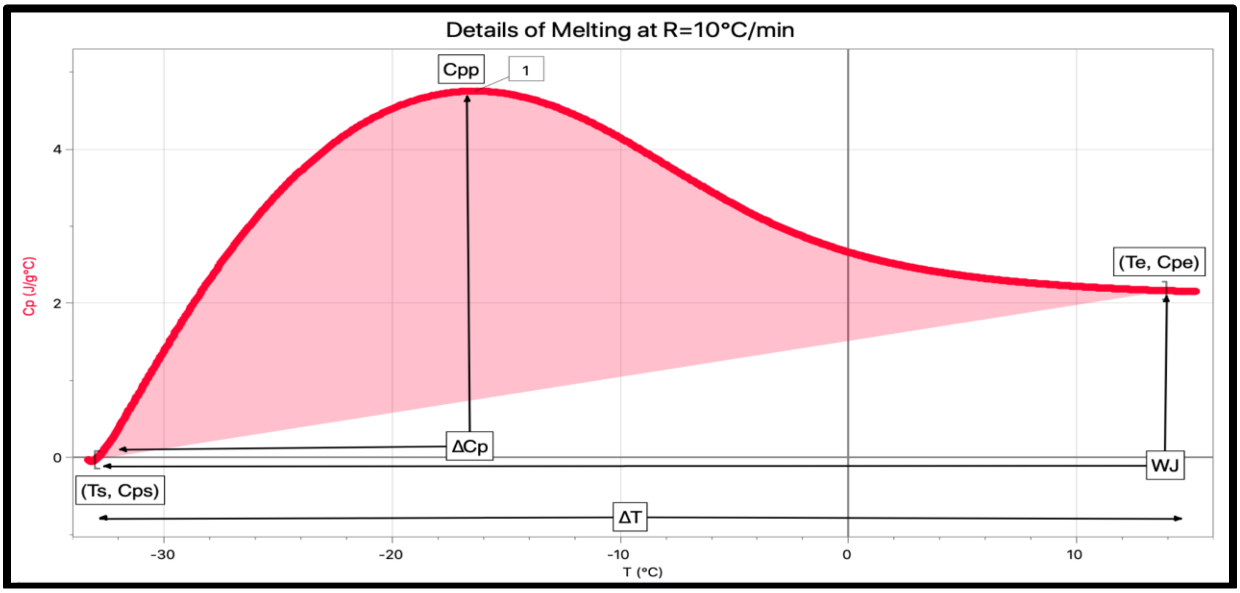

Figure 17. Cp Vs T for endothermic Melting peak of heating 5CB + 7CB mixture at R=10°C/min.

Figure 17 is an expanded melting phase transition peak in heating from Figure 9 and shows features like starting and ending temperatures and specific heat capacities, wing jump and change in temperature of the melting phase transition at R=10°C/min. The pink area denoting the peak integral provides the amount of thermal energy absorbed by the binary sample in order to undergo the melting transition as 96.27 J/g as seen in Table 2.

An amplified nematic phase transition in heating from Figure 9 at R=10°C/min is seen in Figure 18 and shows starting and ending temperatures and specific heat capacities, change in temperature and wing jump of the transition in Table 3. The peak had an area or integral value of 4.49 J/g, being the amount of thermal energy absorbed by the binary sample in order to accomplish the nematic transition as seen in Table 3, represented by the pink peak area.

Figure 19 shows starting and ending temperatures and specific heat capacities, change in temperature and wing jump of the enlarged nematic phase transition of the BLCS in cooling at R=10°C/min from Figure 9. The blue area representing the peak integral has an area of 4.58 J/g as seen in Table 4, and that area gives the quantity of thermal energy released by the binary sample in order to follow through with the nematic transition.

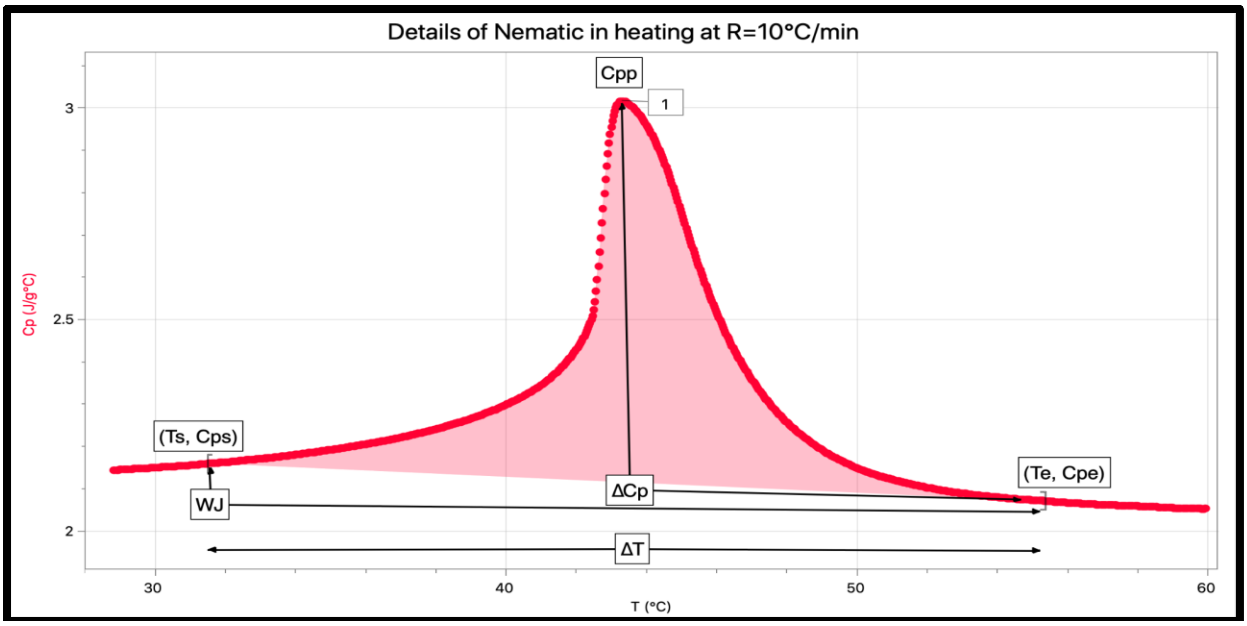

Figure 18. Cp Vs T for endothermic Nematic peak of heating a 5CB + 7CB mixture at R=10°C/min.

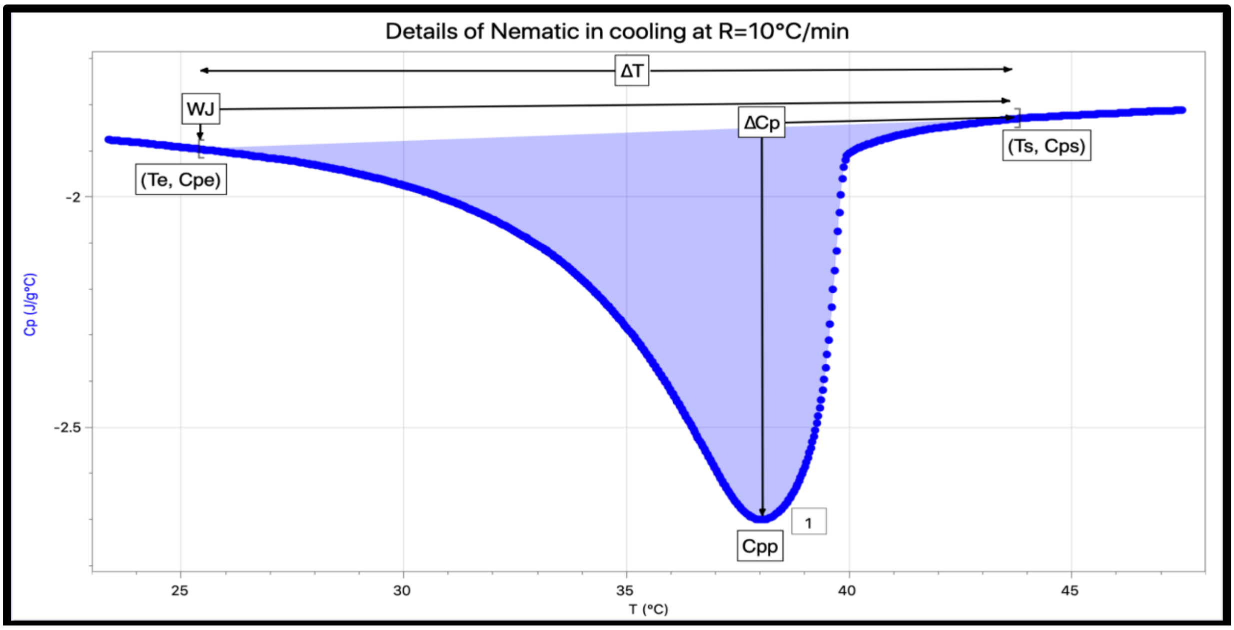

Figure 19. Cp Vs T for exothermic Nematic peak of cooling a 5CB + 7CB mixture at R=10°C/min.

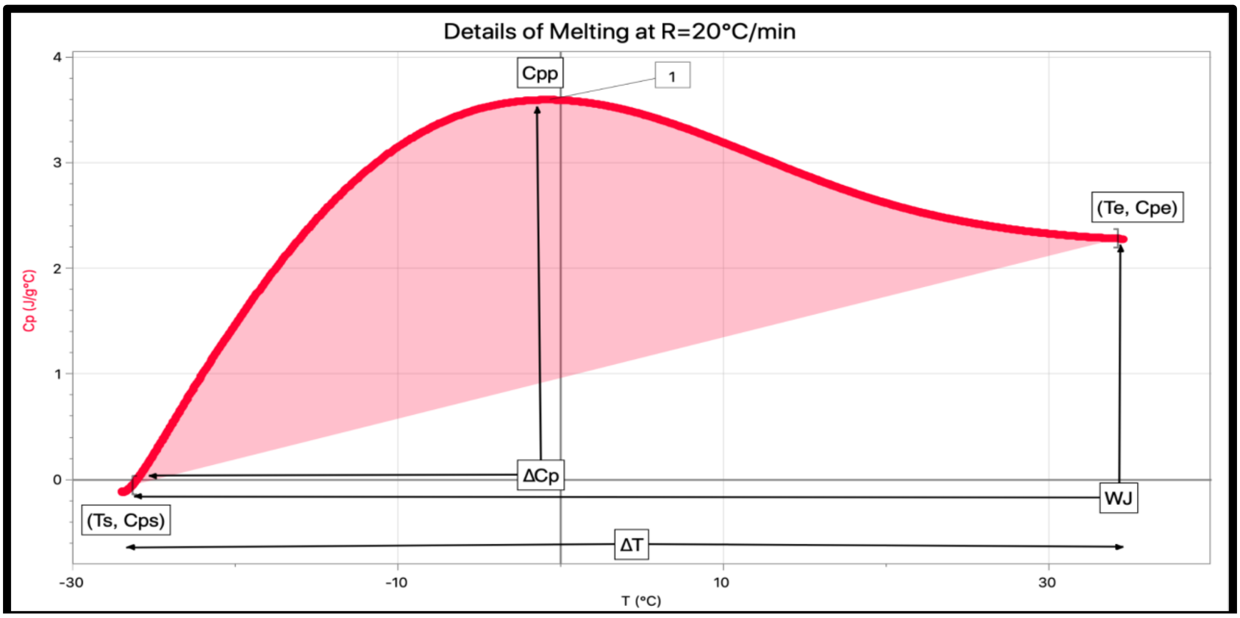

Figure 20. Cp Vs T for endothermic Melting peak of heating a 5CB + 7CB mixture at R=20°C/min.

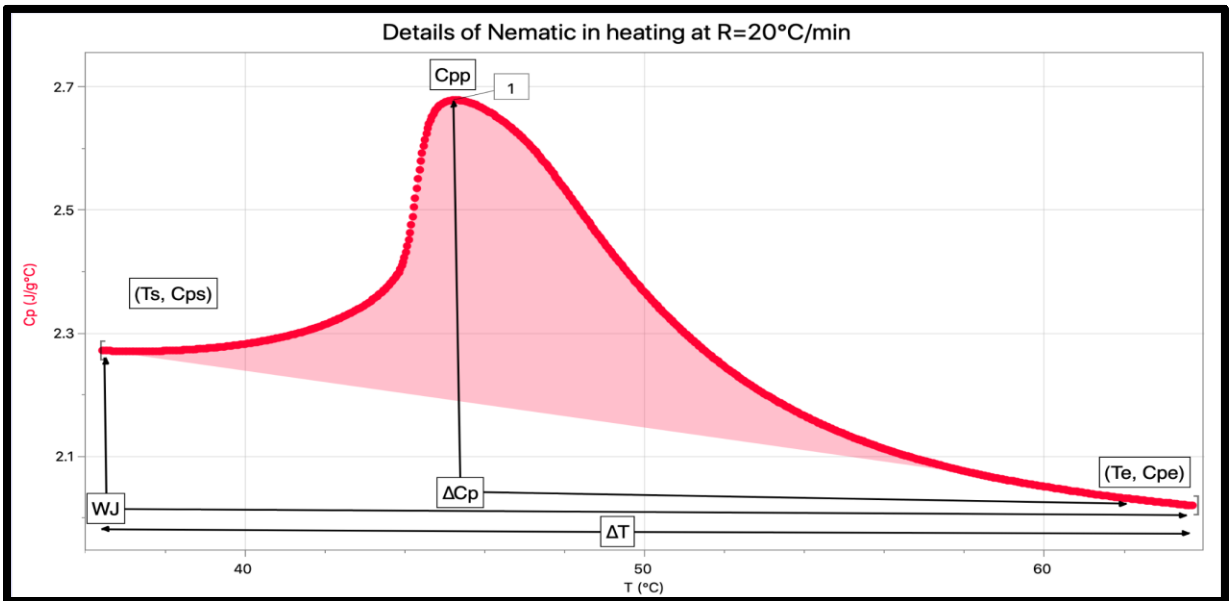

Figure 21. Cp Vs T for endothermic Nematic peak of heating a 5CB + 7CB mixture at R=20°C/min.

Figure 20 shows a zoomed-in melting phase transition in heating from Figure 10 at R=20°C/min and displays starting and ending specific heat capacities, temperatures, wing jump and change in temperature of the transition. The area in pink has a value of 93.38 J/g as seen in Table 2, this peak integral gives the quantity of thermal energy absorbed by the binary sample in order to undergo the melting transition.

Figure 21 is an enlarged version of Figure 10 to show the nematic phase transition in heating at R=20°C/min with starting and ending temperatures and specific heat capacities, change in temperature and wing jump of the transition. The peak integral has a value of 3.23 J/g and is highlighted by the pink area as seen in Table 3, and quantifies the thermal energy absorbed by the binary sample in order for the nematic transition to occur.

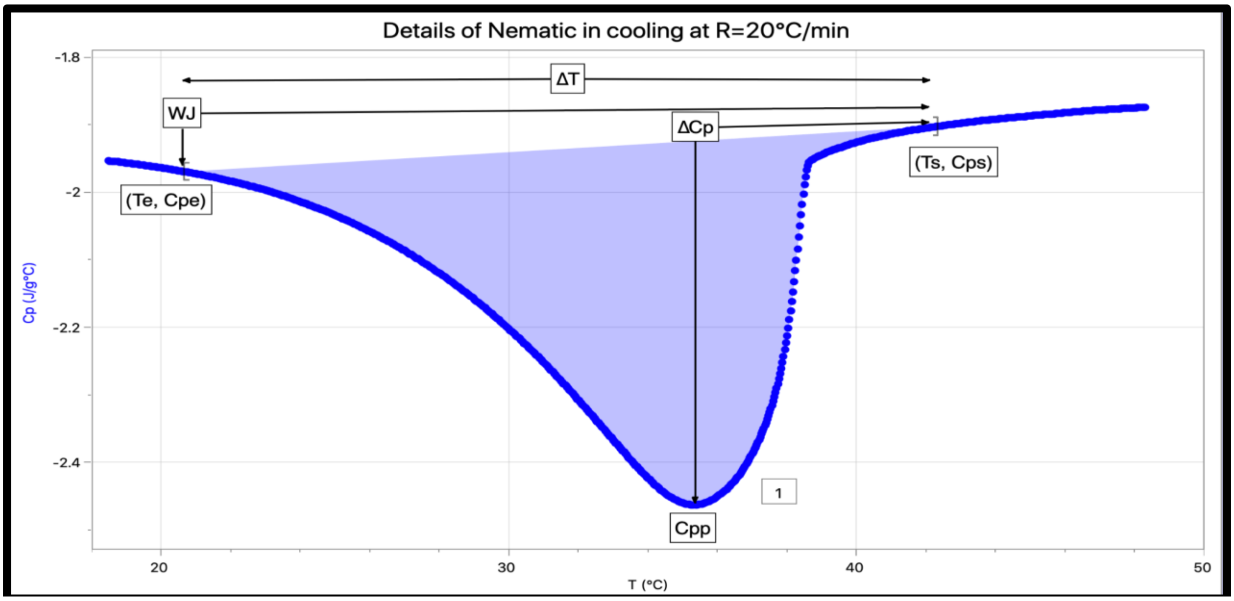

Figure 22. Cp Vs T for exothermic Nematic peak of cooling 5CB + 7CB mixture at R=20°C/min.

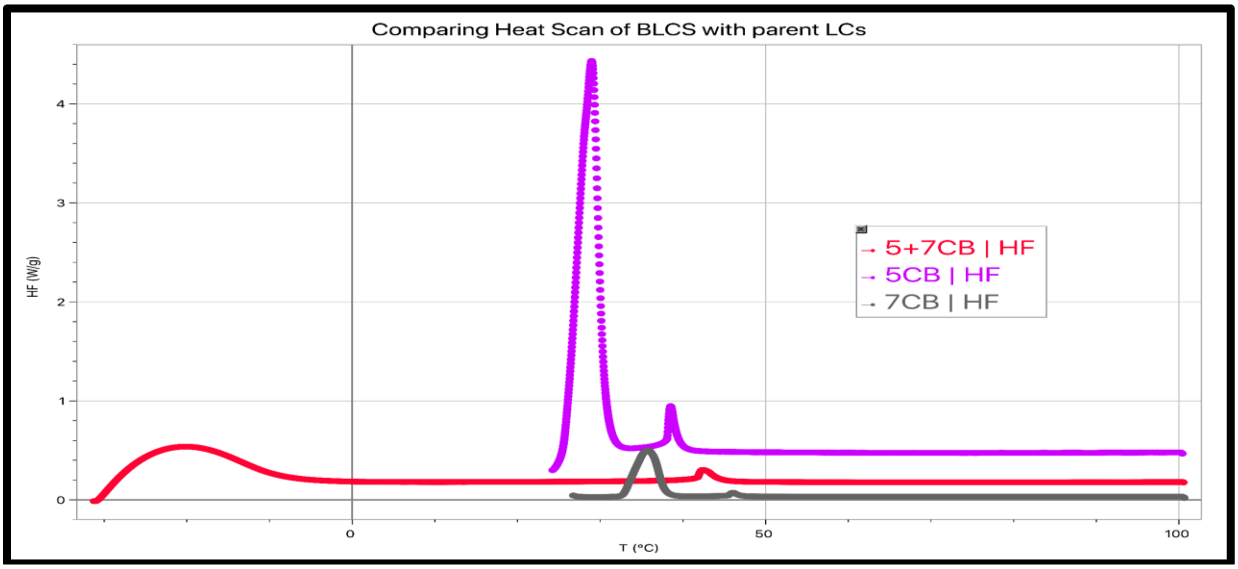

Figure 23. HF Vs T of Melting and Nematic phase transitions during Heating of a 5CB and 7CB BLCS at R=5°C/min, compared with pure component LC heating scans.

Figure 22 is an amplified version of Figure 10 to show the nematic phase transition of BLCS in cooling at R=20°C/min. The blue area representing the peak integral suggests the quantity of thermal energy released by the binary sample in order to complete the nematic transition was 4.57 J/g shown in Table 4.

The presence of two upward endothermic peaks in each sample's heating scan seen in Figure 23 represents the melting and nematic transitions, and the distance between these two transitions is the nematic range (R_N) in heating. This plot displays the massive increase in heating nematic range seen with the 5CB and 7CB BLCS compared to its pure 5CB and 7CB sample ranges.

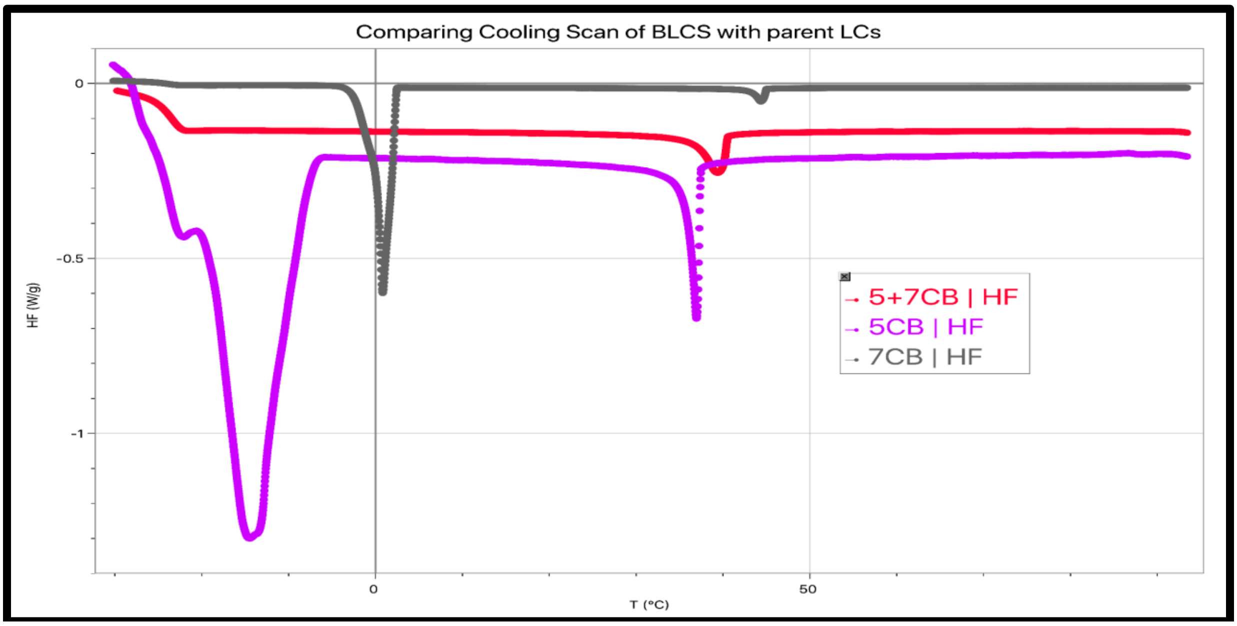

Figure 24. HF Vs T of Nematic and Crystallization phase transitions during Cooling of a 5CB and 7CB BLCS at R=5°C/min, compared with pure component cooling scans.

The two downward exothermic peaks in both pure 5CB and 7CB cooling scans combined with the absence of the crystallization transition in the 5CB and 7CB BLCS proves that the nematic range in cooling also increases when mixing. The nematic range is unknown for the BLCS because the DSC scan did not go low enough in temperature to visualize the crystallization transition, can be seen in Figure 24.

III. DISCUSSION

It is clear from Table 1 that between a 5CB + 7CB BLCS and its pure component LCs 5CB and 7CB, that the Nematic peak temperature for BLCS in heating and cooling is found intermediate and higher than 5CB but the peak temperature of melting transition is much lower than 5CB and 7CB as seen in Figure 23. The melting transition temperature for 5CB and 7CB were T_M= 28.97°C and T_M= 35.78°C, whereas the melting temperature for the BLCS was much lower at T_M= -20.23°C, compared in Figure 25. This widens the nematic range in heating to R_N= 59.73°C, providing LC state in a wider temperature range, because the heating and cooling nematic transition temperatures do not vary too much between these samples.

Figures 26-28 displays the intermediate nature of heating and cooling nematic ΔH, Wing jump, Cpp, and ΔCp data for the BLCS with the exception of ΔH* being higher than both pure 5CB and 7CB samples. This data for the 5CB + 7CB BLCS is organized in Tables 2-4 and compared to the pure component LCs 5CB and 7CB in Tables 5-7. In terms of internal energy change during the heating nematic transition at R=10°C/min, the pure 5CB sample gave an energy change of 1.50 J/g, our BLCS had a change of 4.49 J/g and pure 7CB sample changed by 12.02 J/g. In cooling, pure 5CB changed by 1.62 J/g, the BLCS had an energy change of 4.58 J/g and pure 7CB did by 8.33 J/g. In both cases the BLCS has intermediate properties, but it had a higher total internal energy change while heating of 545.2 J/g compared to pure 5CB and 7CB at 221.8 J/g and 101.5 J/g respectively.

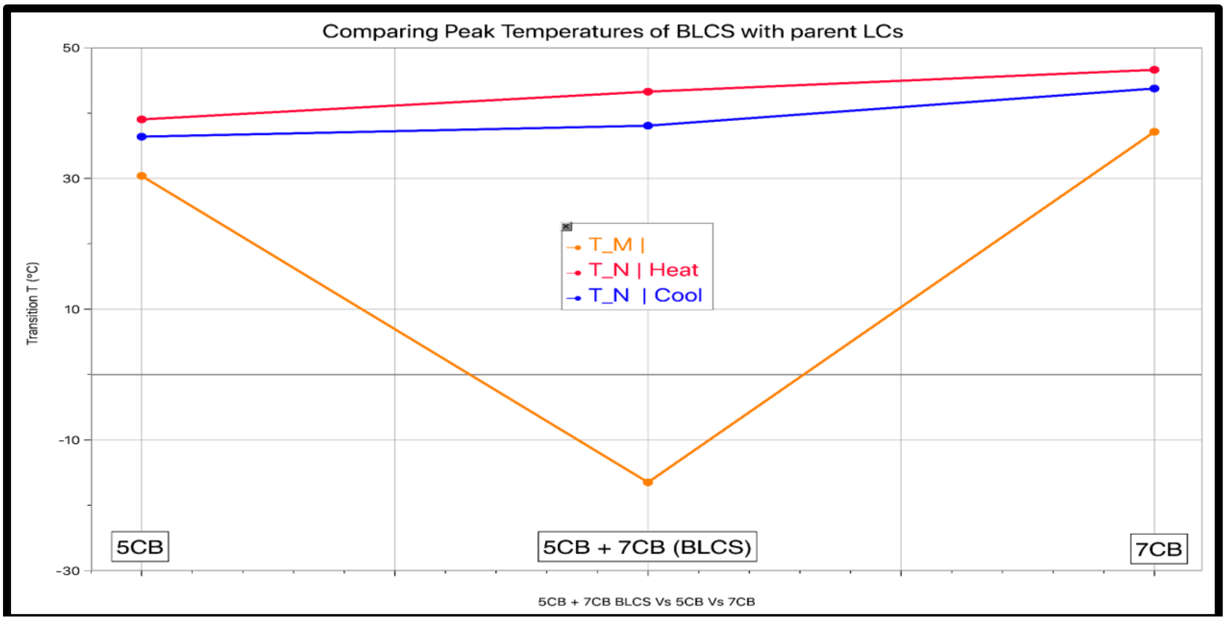

Figure 25. Melting and Nematic transition temperatures of the BLCS and pure component LCs 5CB and 7CB at R=10°C/min.

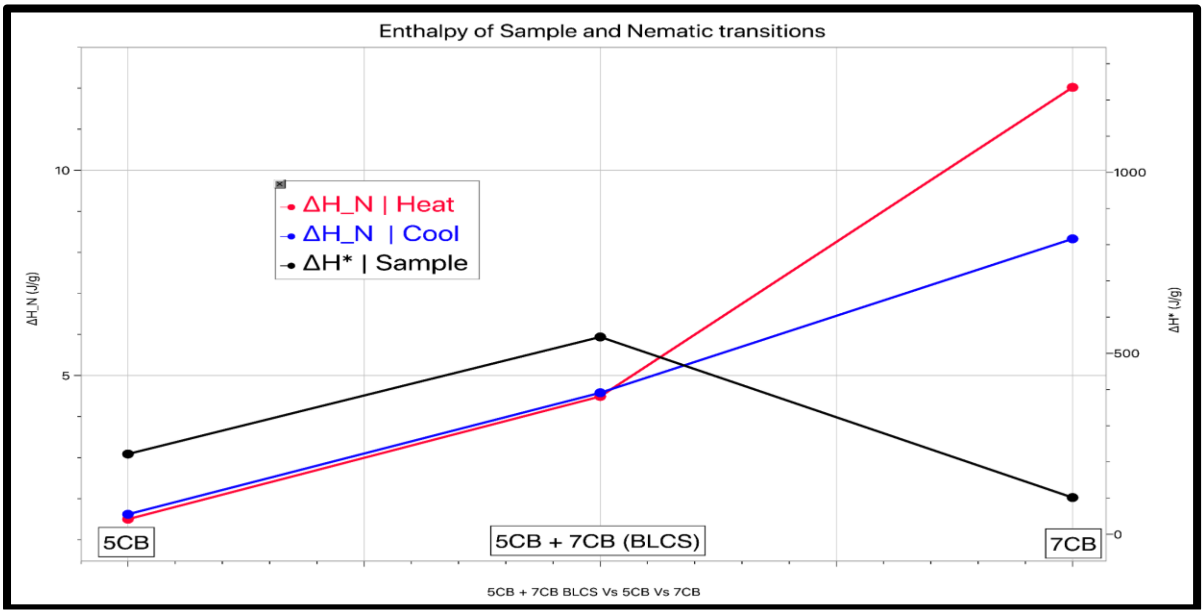

Figure 26. Enthalpy of Nematic transitions in both heating and cooling scans and total internal energy change of the BLCS compared with parents 5CB and 7CB at R=10°C/min.

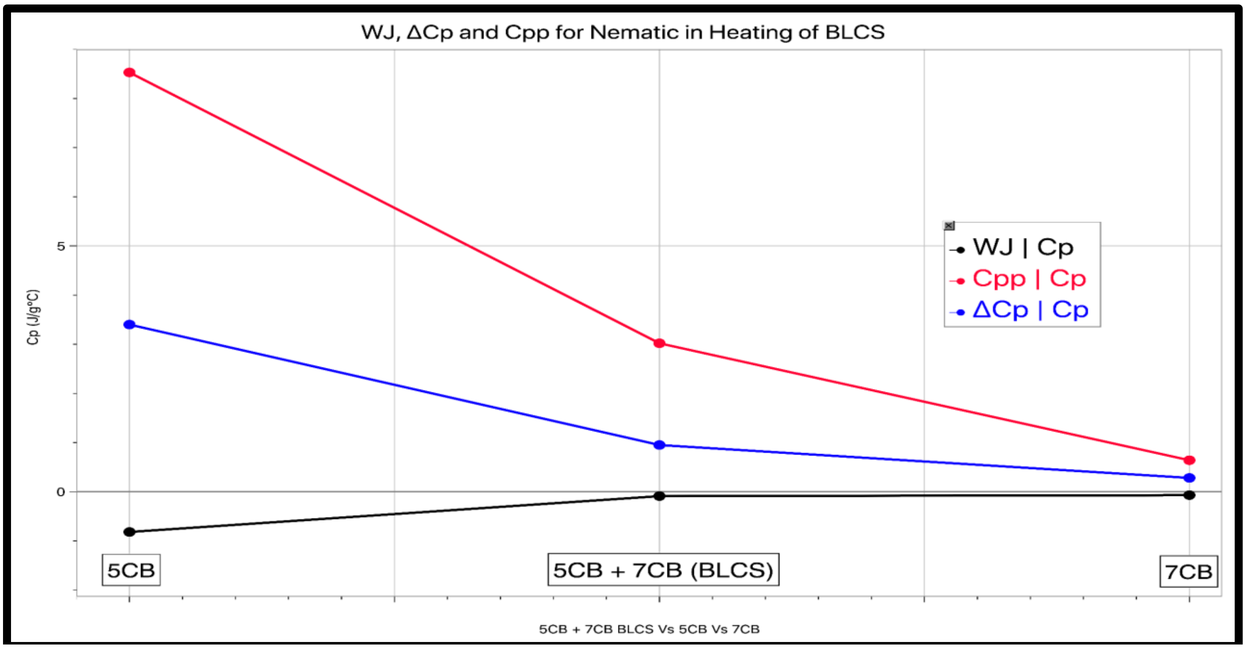

Figure 27. Comparison of WJ, ΔCp and Cpp in heating nematic transition of the BLCS with pure samples of 5CB and 7CB at R=10°C/min.

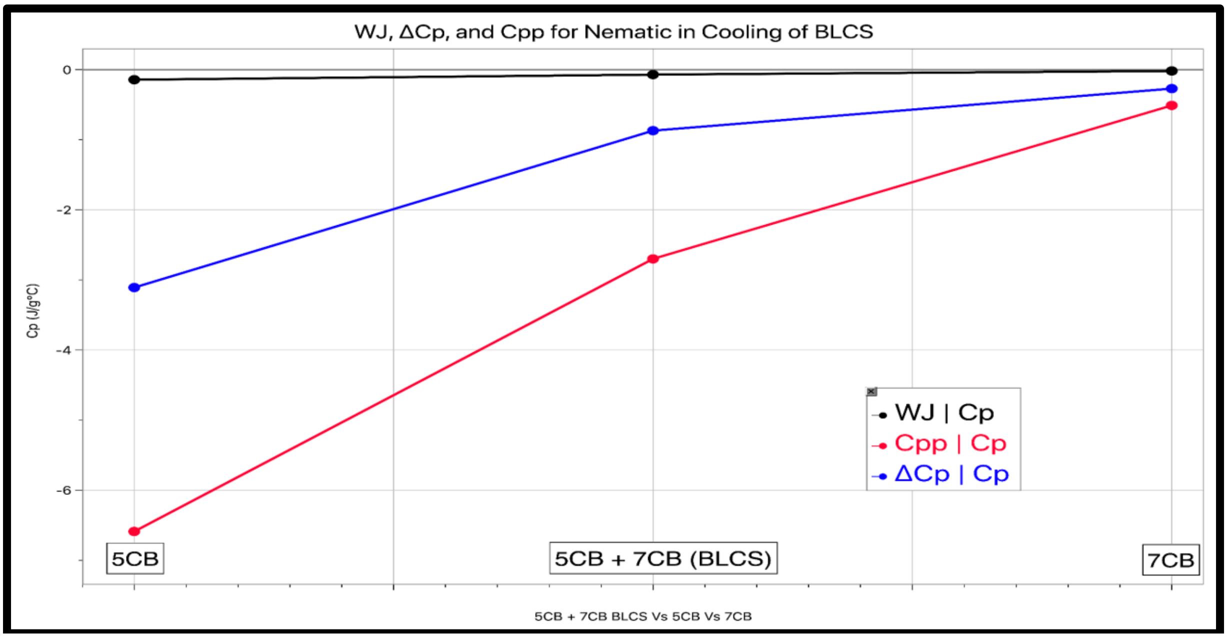

Figure 28. Comparison of WJ, ΔCp and Cpp in cooling nematic transition of the BLCS with pure samples of 5CB and 7CB at R=10°C/min.

The intermediate characteristics between parent LCs continues for thermal qualities like Wing Jump, Cpp and ΔCp for both heating and cooling as seen in Table 7 and Figures 27 and 28. In heating, pure 5CB had a WJ of -0.65 J/g°C while the BLCS had WJ -0.09 J/g°C which was lower than 7CB's WJ at -0.07 J/g°C. The Cpp for 5CB in heating was 8.53 J/g°C, which was higher than the BLCS Cpp 3.02 J/g°C, which was higher than 7CB's Cpp 0.64 J/g°C. Similarly, the ΔCp for the BLCS 0.95 J/g°C falls between that of 5CB and 7CB at 3.4 J/g°C and 0.28 J/g°C respectively.

The intermediate trend of our 5CB + 7CB BLCS between its pure component's thermodynamic characteristics ends when it comes to ΔT and R_N. Shown in Figure 29 and Tables 6 and 7 the BLCS has a higher ΔT and R_N in both heating and cooling than its pure component LCs 5CB and 7CB. In heating, 5CB had the shortest ΔT=5.68°C and R_N=8.64°C, then 7CB at ΔT=6.69°C and R_N=9.50°C, and the BLCS had the largest ΔT=23.81°C and R_N=59.73°C. A similar trend was seen in cooling nematic transitions but this time 7CB had the shortest ΔT=7.42°C and R_N=48.19°C, then 5CB at ΔT=9.95°C and R_N=53.20°C, and the BLCS had the largest ΔT=18.38°C and R_N=62.17°C. The cooling nematic range for the BLCS is an estimate as the crystallization was never observed in cooling, so the nematic range is at least 62.17°C for the BLCS.

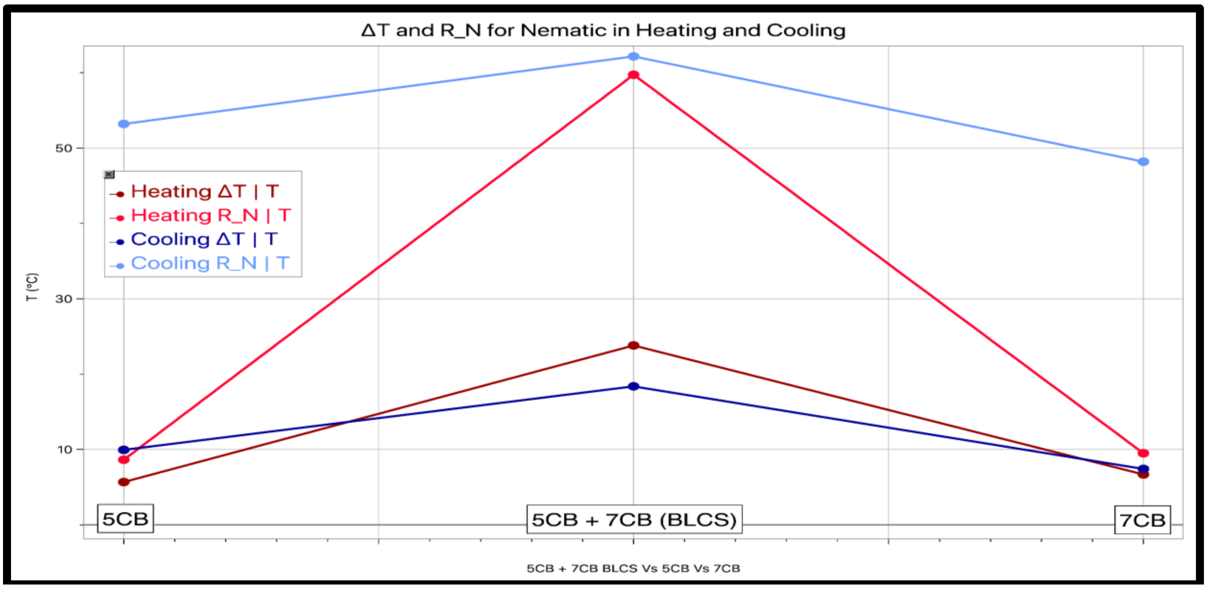

Figure 29. ΔT of Nematic phase transitions and R_N in heating and cooling of BLCS at R=10°C/min, compared with pure samples of 5CB and 7CB.

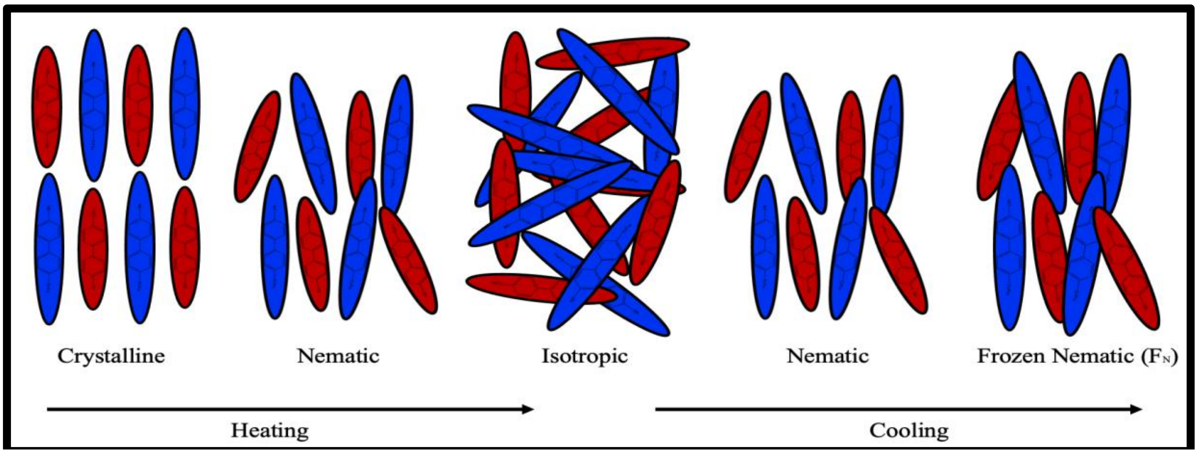

Figure 30. Predicted progression of 5CB + 7CB BLCS phases due to tangling phenomena that caused an absence of crystallization in cooling of BLCS.

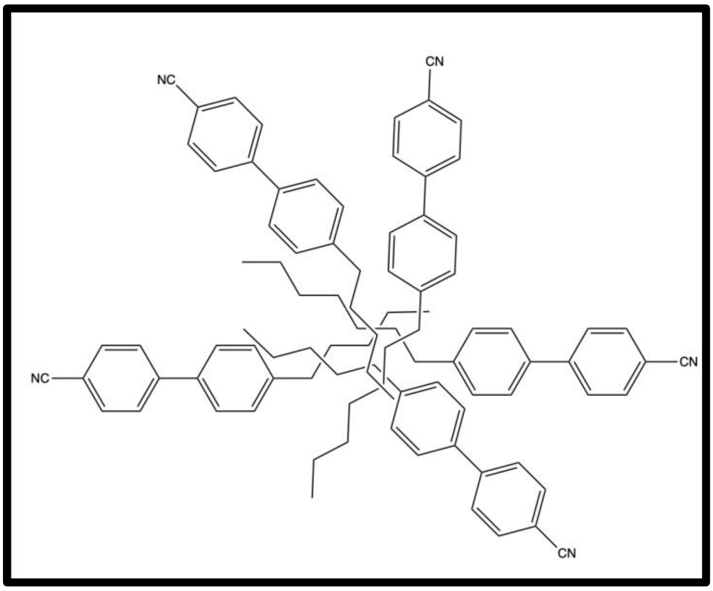

Figure 31. Skeletal structure depiction of 5CB and 7CB molecules tail's tangling causing the frozen nematic phenomenon.

Figure 30 shows the predicted typical phases of BLCS. During heating it goes from crystallization to Isotropic but when it is cooled, it goes to nematic from isotropic but never goes to crystallization. The reason can be seen from the Figure 30 that two different sizes of LC molecules are not able to form ordered state when they cooled down and hence go to frozen nematic state instead if crystallization state. This can happen due to tangling of 5CB and 7CB molecules together and creating a disordered state while cooling down as shown in Figure 31.

DATA TABLES:

The details of data collected and plotted in the result section and the summary drawn from figures plotted in the result section can be seen in this section of Data Tables. All detailed results of BLCS is given in these tables.

In all tables from Table 1-7, the symbols used have these meanings. The T_M, heating T_N, and cooling T_N represent the temperatures where melting, heating nematic, and cooling nematic phase transitions occurred. These transition temperatures create a certain range over which the nematic state is present between melting and nematic transitions, called as Nematic range, denoted by R_N for heating and cooling. The ΔH^* each sample displays the total internal energy change or stored in the sample during heat and cool run for that ramp rate.

The T_s, T_e, C_{ps}, and C_{pe} represent starting and ending temperature and specific heat capacity values for each individual transition. The ΔT and ΔCp denote the change in temperature or specific heat capacity to achieve each phase transition, and the Cpp refers to the maximum specific heat capacity needed for transition. The WJ shows how much the energy level of the DSC sample changed during transition, and the ΔH provides the enthalpy of the phase transition which mean how much energy is either absorbed or released during that transition using DSC.

Table 1. Melting, Nematic Transition Temperatures, Nematic Ranges and Total internal energy change of the BLCS compared to pure component 5CB and 7CB LCs.

LC Sample	**5CB + 7CB (BLCS)**			**5CB**	**7CB**
Rate (°C/min)	5	10	20	5	5
T_M (°C)	-20.23	-16.49	-0.79	28.97	35.78
Heating T_N (°C)	42.33	43.27	45.15	38.52	46.05
Cooling T_N (°C)	39.41	38.07	35.32	36.96	44.36
Heating R_N (°C)	62.56	59.73	45.94	9.55	10.27
Cooling R_N (°C)	69.51*	62.17*	55.12*	51.43	43.52
ΔH* (J/g°C)	545.2			221.8	101.5

Table 2. Details of Melting Transition in heating of 5CB + 7CB BLCS at three different rates

Melting Transition Peaks									
Rate (°C/min)	**T_s (°C)**	**T_e (°C)**	**ΔT (°C)**	**C_{ps} (J/g°C)**	**C_{pe} (J/g°C)**	**C_{pp} (J/g°C)**	**ΔCp (J/g°C)**	**ΔH (J/g)**	**WJ (J/g°C)**
5	-31.18	0.18	31.36	-0.16	2.21	6.45	4.24	91.99	2.37
10	-33.03	13.96	46.99	-0.025	2.17	4.76	2.59	96.27	2.20
20	-26.33	34.24	60.57	-0.05	2.28	3.60	1.32	93.38	2.33

Table 3. Details of Nematic Transition in the heating of 5CB + 7CB BLCS at three different rates.

Heating Nematic Transition Peaks									
Rate (°C/min)	**T_s (°C)**	**T_e (°C)**	**ΔT (°C)**	**C_{ps} (J/g°C)**	**C_{pe} (J/g°C)**	**C_{pp} (J/g°C)**	**ΔCp (J/g°C)**	**ΔH (J/g)**	**WJ (J/g°C)**
5	31.97	49.10	17.13	2.25	2.18	3.63	1.45	4.21	-0.07
10	31.53	55.34	23.81	2.16	2.07	3.02	0.95	4.49	-0.09
20	36.42	63.71	27.29	2.27	2.02	2.68	0.66	3.39	-0.25

Table 4. Details of Nematic Transition in the cooling of 5CB + 7CB BLCS at three different rates.

Cooling Nematic Transition Peaks									
Rate (°C/min)	**T_s (°C)**	**T_e (°C)**	**ΔT (°C)**	**C_{ps} (J/g°C)**	**C_{pe} (J/g°C)**	**C_{pp} (J/g°C)**	**ΔCp (J/g°C)**	**ΔH (J/g)**	**WJ (J/g°C)**
5	43.51	28.93	14.58	-1.72	-1.78	-3.06	1.34	4.30	-0.06
10	43.81	25.43	18.38	-1.83	-1.90	-2.70	0.87	4.58	-0.07
20	42.34	20.68	63.02	-1.90	-1.97	-2.46	0.56	4.57	-0.07

Table 5. Wing Jump (WJ) comparison for each transition between BLCS and its parent - pure component LCs 5CB and 7CB.

Wing Jump (J/g°C) at R= 10°C/min			
	5CB + 7CB (BLCS)	**5CB**	**7CB**
T_M	2.20	1.48	0.143
Heat T_N	-0.09	-0.65	-0.07
Cooling T_N	-0.07	-0.21	-0.02

Table 6. Comparison of Thermodynamic behavior of the 5CB + 7CB BLCS to its parents - pure component LCs during Heating Nematic transition

R= 10°C/min	**5CB + 7CB (BLCS)**	**5CB**	**7CB**
ΔH (J/g)	4.49	1.50	12.02
ΔH* (J/g)	545.2	221.8	101.5
WJ (J/g°C)	-0.09	-0.65	-0.07
Cpp (J/g°C)	3.02	8.53	0.64
ΔT (°C)	23.81	5.68	6.69
ΔCp (J/g°C)	0.95	3.4	0.28
R_N (°C)	59.73	8.64	9.50

Table 7. Comparison of Thermodynamic behavior of the 5CB + 7CB BLCS to its parents - pure component LCs during Cooling Nematic Transition

R= 10°C/min	**5CB + 7CB (BLCS)**	**5CB**	**7CB**
ΔH (J/g)	4.58	1.62	8.33
ΔH* (J/g)	545.2	221.8	101.5
WJ (J/g°C)	-0.07	-0.21	-0.02
Cpp (J/g°C)	-2.70	-6.59	-0.51
ΔT (°C)	18.38	9.95	7.42

ΔCp (J/g°C)	-0.87	-3.109	-0.27
R_N (°C)	62.17*	53.202	48.19

IV. CONCLUSION

This paper shows some unique behavior of a next generation "Binary Liquid Crystal System (BLCS)" using DSC technique. Based on data shown in the data section and the Figure 30-31, We can conclude our results in the favor of using this BLCS in LCDs or saying that this BLCS can be useful in LCDs. Due to having seven carbons compared to five carbons in its carbon tail, 7CB molecules are larger and weigh more than 5CB molecules. When the two are mixed in 1:1 by weight percent to make a 5CB + 7CB BLCS and placed in a DSC to undergo heating, the mixture fails to produce a crystallization in cooling. Likely because the different sized LCs try to reform a lattice crystal structure as heat is removed but do not fit well together due to their size difference. Each LC's carbon tails get tangled with each other causing the nematic state to exist at much lower temperatures. This failure of order increases the disorder range and nematic range in cooling of the BLCS. In fact, it may be possible to cool this BLCS to low temperatures to solidify to a rubbery or non-crystalline state but never reach a crystalline state. Or the DSC instrument used for study may not go to very low temperature range to provide such a temperature range where BLCS can be crystallized again.

The observed increase in nematic range of the 5CB + 7CB BLCS in both heating and cooling compared to its parent LCs proves its significance in LCDs enabling nematic phase transition over a wider temperature range. In addition to the increase in temperature range where the BLCS is viable, the intermediate nature of the BLCS's enthalpy, or energy absorbed for either nematic transition, suggests the mixture displays some thermal characteristics of both parent LCs. Similar to the WJ, Cpp and ΔCp, which all gave intermediate values shown in tables above in the result section for the BLCS. This shows that BLCS has several thermal properties like its parents but some of them are unique and out of range of its parents. The total internal energy change of the BLCS during heating was greater than both the total internal energy changes of the pure parent component LCs 5CB and 7CB combined. This suggests that although the individual nematic phase transitions of the BLCS display intermediate thermal behavior, the overall heating and cooling use much more energy and give higher nematic range in heating and cooling both. This unique behavior of BLCS makes it more useful in the LCD world.

ACKNOWLEDGEMENT

We like to thank Professor John C. MacDonald, Chemistry and Biochemistry department, and Andrew Butler from Life Sciences and Bioengineering Center, WPI, Worcester, MA for providing help with the Differential Scanning Calorimetry instrument. We also like to acknowledge NETZSCH company for their DSC 214 instruments, and pans and lids. The student author likes to thank Dr. Dipti Sharma for supervising this research internship with Liquid Crystal, and Emmanuel College for running internship programs.

REFERENCES

[1]. What Are Liquid Crystals? (n.d.). Kent State University. Retrieved October 31, 2022, from https://www.kent.edu/amlci/what-are-liquid-crystals
[2]. Wikipedia contributors. (2022, October 30). Liquid crystal. Wikipedia. https://en.wikipedia.org/wiki/Liquid_crystal
[3]. New Vision Display. (2018, May 30). What is "liquid crystal"?https://www.newvisiondisplay.com/liquid-crystal/
[4]. Libretexts. (2020, August 15). Liquid Crystals. Chemistry LibreTexts. https://chem.libretexts.org/Bookshelves/Physical_and_Theoretical_Chemistry_Textbook_Maps/Supplemental_Modules_(Physical_and_Theoretical_Chemistry)/Physical_Properties_of_Matter/States_of_Matter/Liquid_Crystals
[5]. Contributor, T. (2019, September 13). LCD (Liquid Crystal Display). WhatIs.com. Retrieved September 26, 2022, fromhttps://www.techtarget.com/whatis/definition/LCD-liquid-crystal-display
[6]. LCD Definition (Liquid Crystal Display). (2021, September 30). Lifewire. Retrieved September 26, 2022, fromhttps://www.lifewire.com/what-is-liquid-crystal-display-lcd-2625913
[7]. How The Technology of LCD Displays Works - Xenarc Technologies Blog. (n.d.). Retrieved September 26, 2022, fromhttps://www.xenarc.com/lcd-technology.html
[8]. Tyson, J., & Carmack, C. (2021, September 16). How Computer Monitors Work. HowStuffWorks. Retrieved September 26, 2022, from https://computer.howstuffworks.com/monitor5.htm
[9]. Seide, M., Doran, M. C., & Sharma, D. (2022). Analyzing Nematic to Isotropic (N-I) Phase Transition of nCB Liquid Crystals Using Logger Pro. European Journal of Applied Sciences, 10(3), 98–124. https://doi.org/10.14738/aivp.103.12373
[10]. Sharma, D., & Mello, J. (2022). Details of Nematic Phase Transition and Nematic Range of 5OCB Liquid Crystal using Logger Pro. International Journal of Research in Engineering and Science (IJRES), 10(9), 197–217.
[11]. Sharma, D., & Doran, M. (2022). Reporting Strange and Unique Behavior of 4CB Liquid Crystal using Logger Pro. International Journal of Research in Engineering and Science (IJRES), 10(5), 27–41.
[12]. Sharma, D., & Mello, J. (2022a). Effect of Reheating and Ramp Rates on Phase Transitions of 5OCB Liquid Crystal using Logger Pro. International Journal of Research in Engineering and Science (IJRES), 10(9), 218–236.
[13]. Sharma, D., MacDonald, J. C., &Iannacchione, G. S. (2006, August 1). Thermodynamics of Activated Phase Transitions of 8CB: DSC and MC Calorimetry. The Journal of Physical Chemistry B, 110(33), 16679–16684.

[14]. Sharma, D. (2010, May 18). Non-isothermal kinetics of melting and nematic to isotropic phase transitions of 5CB liquid crystal. Journal of Thermal Analysis and Calorimetry, 102(2), 627–632.https://doi.org/10.1007/s10973-010-0837-2

[15]. Oweimreen, G., &Morsy, M. (2000). DSC studies on p-(n-alkyl)-p′-cyanobiphenyl (RCB's) and p-(n-alkoxy)-p′-cyanobiphenyl (ROCB's) liquid crystals. Thermochimica Acta, 346(1–2), 37–47. https://doi.org/10.1016/s0040-6031(99)00411-6

[16]. Baumann, C., Marcerou, J., Rouillon, J., & Prost, J. (1984). Pre-transitional effects in isotropic phases close to nematic, nematic discoid and columnar phases. Journal De Physique, 45(3), 451–458. https://doi.org/10.1051/jphys:01984004503045100

[17]. Differential scanning calorimetry - how does it work? LinseisMessgeräte GmbH. (2020, November 26). Retrieved March 4, 2022, fromhttps://www.linseis.com/en/methods/differential-scanning-calorimetry-dsc/

[18]. Haines PJ, Reading, M, Wilburn FW. Differential thermal analysis and differential scanning calorimetry. In Brown ME (ed): Handbook of Thermal Analysis and Calorimetry, vol 1. The Netherlands: Elsevier Science BV, 1998;279–361.

[19]. Seide, M., Doran, M. C., & Sharma, D. (2022). Analyzing Nematic to Isotropic (N-I) Phase Transition of nCB Liquid Crystals Using Logger Pro. European Journal of Applied Sciences, 10(3), 98–124. https://doi.org/10.14738/aivp.103.12373

[20]. Sharma, D., & Mello, J. (2022). Details of Nematic Phase Transition and Nematic Range of 5OCB Liquid Crystal using Logger Pro. International Journal of Research in Engineering and Science (IJRES), 10(9), 197–217.